Submitted to Neues Jahrb. Mineral. Monatsh. (6.3.87)

Jahresbericht

N. Jahrb. Mineral. Monats

MRF/371

An evaluation of fluid inclusion decrepitometry using quartz from the Kingsgate molybdenite–bismuth deposits, New South Wales, Australia

By George Hladky and Ronald W.T. Wilkins, North Ryde

With 5 figures and 2 tables in the text

Authors' address: CSIRO Division of Mineral Physics and Mineralogy, PO Box 136, North Ryde, 2113, NSW, Australia.

Abstract: A study has been made of the relationship between heating-freezing stage and decrepitation data for fluid inclusions in three growth zones of a large quartz crystal from Kingsgate, New South Wales, Australia. It was found that the mean homogenization temperatures can be estimated from the decrepitation data either by specific corrections related to the known inclusion salinity (more precise) or by a general correction which is independent of salinity (less precise). Discrepancies of up to 30-40°C exist between the actual and estimated homogenization temperatures. Of the several possible reasons for these discrepancies the most likely is that the inclusion size affects the temperature of decrepitation.

Key words: Fluid inclusions, decrepitometry, quartz, mineralization, molybdenite, bismuth.

Introduction

Decrepitometry is a method of characterizing mineral samples by the discrete acoustic emissions they produce on heating. These emissions originate in the fracturing and leaking of fluid inclusions. The method can rapidly provide a large quantity of semi-quantitative fluid inclusion data in a survey which can be used in such applications as distinguishing mineralized and barren quartz veins (BURLINSON et al., 1983). As part of a program of testing a new approach to the theory and practice of decrepitometry (HLADKY and WILKINS, 1987; WILKINS et al., 1987), we have examined a well characterized quartz crystal from a quartz-molybdenite-bismuth deposit from Kingsgate, New South Wales, Australia. This study provides a clear example of the relationship between acoustic emissions and fluid inclusion content and enables a detailed evaluation of a number of complexities inherent in the technique.

Materials and methods

The sample studied is part of a large crystal 150 mm in length with corroded prismatic and unequally-developed rhombohedral faces. It was cut into two pieces parallel to one of the larger rhombohedral faces in such a way that three growth zones were intersected. A 7 mm thick slice from one of the cut surfaces was sufficient to provide material both for a polished thin section and crushed samples for decrepitometry. Fig. 1 indicates the location of the samples from the three zones selected for study.

The blocks for decrepitometry were crushed in a small roller mill and sieved into 1000-600, 600-425, 425-212, 212-106 and 106-53 μm fractions. The samples (0.5 g) were run in a newly-designed microprocessor-controlled decrepitometer, constructed by Burlinson Geochemical Services Pty. Ltd., at a heating rate of 20°C/min over the range 100-600°C. The results, which are displayed by the instrument in the form of a histogram of the number of counts per 10°C interval over this temperature range, were then treated on a PDP 11 computer using GAUSS, a curve fitting program which utilizes the subprogram MINIM by D.E. Shaw of the CSIRO Division of Mathematics and Statistics, Sydney, Australia. With this program the curves are resolved into a selected number of Gaussian peaks and the number of counts, mean temperature and standard deviation are tabulated for each peak. The results were then plotted with a Hewlett Packard 7221C plotter.

The thin sections were examined for indications of origin of the inclusions. To determine size distributions, 200 inclusions were selected from each zone using random simultaneous x and y translations of the section on a moving microscope stage. At each position the inclusion closest to the crosswires of the microscope was measured for length and width.

Portions of the thin sections were then cut out for homogenization temperature and salinity determinations using a SGE heating-freezing stage. The stage was calibrated at the triple point of CO_2 (-56.6°C) using a CO_2 inclusion standard, and at the melting points of pure water, $NaNO_3$ (306.8°C) and $K_2Cr_2O_7$ (398°C). At 0°C and below the errors are believed to be ± 0.2°C and in the region of most of the homogenization temperature measurements (200-400°C) the error should be within ± 5°C.

Results

Fluid inclusion distribution

In the section of the outer zone of the crystal a substantial proportion of the inclusions are roughly arranged parallel to a rhombohedral crystal face (Fig. 1) and are primary in origin. Other inclusions not zonally arranged but lying along non-intersecting curved surfaces could also be primary inclusions of the lineage boundary type. Inclusions in the intermediate zone are not zonally arranged but again are mainly to be found along well-defined curved surfaces, very few of which actually intersect one another within the thickness of the section. The inclusions in the core are distributed both irregularly and along well-defined intersecting healed fracture surfaces. It is probable that both primary and pseudosecondary inclusions are present in this zone but because the origin of many inclusions was not clear they were not classified at the time of data collection. The inclusions in this crystal show very little evidence of necking-down. Low density fluids such as may have originated by boiling are absent.

Size frequency distribution data for inclusions from the three zones are presented in Fig. 2.

Heating-freezing stage

The results of the freezing stage examination of the fluid inclusions from the three zones of the crystal (Fig. 3) show that all inclusions are of relatively low salinity. Two groups of inclusions are nevertheless distinguishable from the rim zone of the crystal, one with a salinity < 1.5 wt.% NaCl equiv. (Tm ice 0.0 to -0.7°C) and the other

with a salinity in the range 4 to 6 wt.% NaCl equiv. (Tm ice -2.5 to -3.5°C). At least some inclusions in the latter group have appreciable gas contents because in these the freezing occurs in two steps and, when all the ice is melted on warming, the bubble still remains deformed until the invisible clathrate melts at approximately +1°C. Inclusions from the intermediate zone of the crystal all have a salinity of less than 1 wt.% NaCl equiv. and there is no evidence of clathrate formation. Inclusions from the core zone fall into two groups on the basis of whether a clathrate is present or not. A clathrate was found in all inclusions with Tm ice -3.6 to -4.5°C. Although the clathrate is invisible, evidence of melting at approximately +9 to +10°C was obtained by observing bubble movement during cycles of freezing and warming to successively higher temperatures. The gas could not be condensed at -130°C and there was no evidence of any phase change in the bubble in the region of the CO_2 triple point (-56.6°C).

Homogenization temperatures obtained from 100 inclusions in each zone are plotted in Fig. 4. Heating and freezing stage results were obtained from different suites of inclusions except for the core sample from which there was an overlap of 25 inclusions for which both heating and freezing data were obtained.

Decrepitation data

Representative decrepigrams for the three zones are compared with the corresponding homogenization temperature histograms in Fig. 4. An attempt to fit the decrepitometric data by two Gaussian curves was successful for the intermediate and rim zones but unsuccessful for the

core samples. These, however, were satisfactorily fitted by three Gaussians. The parameters of the component curves for the five samples from each of the three zones are listed in Table 1.

The effect of particle size of a sample on its decrepitation response is illustrated in Fig. 5 for the different size fractions of the sample from the core of the crystal.

Discussion

Occurrence of crystal

The geology and mineralogy of the Kingsgate quartz-molybdenite-bismuth deposit have been discussed by ANDREWS (1916), GARRETY (1953) and LAWRENCE and MARKHAM (1962). The deposit consists of a number of small irregular pipe-like bodies in the Red Range Granite of Permian age, in proximity to the roof of the intrusion and near the contact with surrounding Carboniferous sediments. The pipes have no brecciation features, but they have a rough zonal structure consisting of a margin of compact granular quartz and bismuth, an intermediate zone consisting of porous granular quartz with disseminated molybdenite and a central zone containing massive molybdenite and coarse granular and well-formed crystals of quartz commonly up to 10-20 cm in size. The crystal selected for the present study was collected from a spoil heap but probably derived from the latter zone.

EADINGTON (1977), in a study of the fluid inclusions of the quartz from the different zones of the pipes, recorded salinities in the range 0- ~10 wt.% NaCl equiv. and homogenization temperatures in the range 210-375°C. Significant variations in the temperature and salinity of

the inclusions were noted even within single crystals, and some of the inclusion fluids were shown to contain a significant gaseous component.

Homogenization temperature-decrepitation temperature correlations

The origin of the decrepitation effect and the general nature of decrepitation curves are discussed in detail in two papers that form the basis of a new approach to the theory and practice of decrepitometry (HLADKY and WILKINS, 1987; WILKINS et al., 1987). Classic Canadian and Russian works are extensively discussed in these papers. A number of important results follow from our new approach. The decrepitation temperature of an inclusion is determined by factors controlling the development of internal pressure with increasing temperature (solution composition and density), the mechanical properties of the mineral and the way they change with temperature, and the size and shape of the inclusion. Relationships between homogenization temperatures and decrepitation temperatures are simple for inclusions larger than a critical dimension which can be shown theoretically to be approximately 15 μm for quartz. The high temperature peak at about 550°C, which varies in intensity but is almost always present in a decrepigram, is associated with changes in the Young's modulus of quartz in the region of the α-β transition and represents the decrepitation of small (<15 μm) inclusions which would otherwise survive to higher pressures.

Relationships between decrepitation and homogenization temperatures and comparisons between different decrepigrams are based on their resolution into a number of Gaussians and on the mean temperature, standard deviation and total counts in the component peaks. The mean

decrepitation temperature (Tdm) and mean homogenization temperature (Thm) are defined and discussed in HLADKY & WILKINS (1987). This analysis procedure is followed in the present paper, though it should be noted that it differs from the classical approach (SCOTT, 1948; SMITH, 1949) based on the identification of the decrepitation temperature as the commencement of the first massive increase in decrepitation activity in a sample.

For the purpose of comparing homogenization and decrepitation results, the high temperature peak associated with the α-β transition may be eliminated from consideration. It is then apparent that the homogenization temperature data and the corresponding decrepitometry data are closely related (Fig. 4). The major differences are in the mean positions of the peaks and in the greater standard deviation of the decrepitometry data. The decrepitation peaks are displaced to higher temperatures because of the increment of overheating which must take place before decrepitation occurs. The rim sample provides an excellent example of the way a very sharp distribution of homogenization temperatures can result in a broad decrepitation response. The broadening results in part from the small range in salinity of the inclusions so that there is a range of appropriate isochores and different rates of pressure increase in the different inclusions on heating. Another factor is that the critical breaking pressure also depends strongly upon the shape of the inclusions. Perhaps most importantly, however, the temperature gradient over that part of the furnace containing the sample results in otherwise identical inclusions decrepitating over a range of measured temperature.

The results of the homogenization temperature determinations (Fig. 4) show that the modal temperature decreases from 355°C in the core through 285°C in the intermediate zone to 255°C in the rim. A strong shoulder is present on the low temperature side of the main peak from the core sample. This shoulder appears to consist of two overlapping homogenization temperature peaks at 285 and 315°C and they are probably represented in the corresponding decrepigrams by the two shoulders at 360 and 390°C best seen in the 212-425 and 425-600 μm fractions of the core zone (Figs. 4 and 5). For the purpose of this analysis we have considered these two peaks to be a single composite peak similar in mean position and standard deviation to the major peaks of the intermediate and rim zones. A possible interpretation of the temperature data from the core is that the high temperature peak originates from primary inclusions and the low temperature peak represents pseudosecondary inclusions formed by the healing of cracks which developed in the core zone of the crystal during the growth of the outer zones with declining temperatures.

HLADKY & WILKINS (1987) show that provided the inclusions are larger than some critical dimension depending on the host mineral, and if the composition of the fluid is not known, a correction of -75 ± 20°C to the mean temperature of a decrepitation peak gives a good estimation of the mean homogenization temperature of a Gaussian population of inclusions within the temperature range 100-400°C. The results of applying this average correction procedure to data from each of the 425-600 μm size fractions are given in Table 2.

As some salinity data are available for the inclusions in this crystal, it should be possible to make more precise corrections by the use of specific isochore information. Results for inclusions from the core sample, from which both heating and freezing data are available, show that those with Tm ice > -2.0°C give rise to the low homogenization temperature peak at 300°C and the apparently more saline inclusions, which also show evidence of clathrate formation, give rise to the intense peak at 350°C. The gas in the latter inclusions is not readily condensed and is most likely to be nitrogen rich. It is present in sufficient quantity to give rise to an important volume of clathrate which increases the apparent salinity of the solution. Until the composition and density of the gas phase are determined, the corresponding isochores cannot be constructed and precise corrections made. However corrections for 1-5 wt.% NaCl solutions give fair to good estimates of the mean homogenization temperatures corresponding to the two decrepitation peaks (Table 2).

Similarly, inclusions from the rim zone fall into two groups with Tm ice > 0.7°C or Tm ice -2.5 to -3.5°C. At least some of the apparently higher salinity inclusions contained invisible gas clathrate so that detailed corrections cannot at present be made for this section of the crystal. Approximate corrections for a 1-5 wt.% NaCl solution can reasonably be applied.

Inclusions from the intermediate zone, however, are more uniform, with Tm ice > 0.4°C and a salinity of approximately 1 wt.% NaCl equivalent. Application of the appropriate correction for this salinity gives an estimated Thm of 303°C whereas the measured mean homogenization

temperature is 276°C. If the inclusion salinity had not been known, application of a general correction would have given an estimated Thm of 310 ± 20°C.

There are several possible reasons for the discrepancies between measured and estimated Thm values.

1. The temperature calibration of the decrepitometer could be in error. As a result of extensive calibration tests we believe that the error for the conditions used should be no greater than ± 10°C.
2. In dry natural quartz the internal pressure of decrepitation for inclusions larger than the critical size (15 μm) could be greater than the experimentally determined 850 bar for synthetic quartz (see discussion in WILKINS et al., 1987).
3. The gas content, even in those inclusions in which the effect of clathrate formation was not observed, may have been such that the pressure was not well approximated by that of the NaCl solution equivalent to the fluid.
4. The sample size for mean homogenization temperature determination (200 inclusions) was inadequate and the decrepitation data based on > 20,000 inclusions are more reliable.
5. As expected from the relationship between inclusion size and critical decrepitation pressure (WILKINS et al., 1987), those inclusions in the sample below critical dimensions could be sufficiently delayed in decrepitation that the peaks are displaced to slightly higher temperatures.

Of the five factors listed, the inclusion size effect is probably the major cause of the discrepancy between the actual and mean

homogenization temperatures. With irregularly shaped inclusions it is difficult to decide on the most appropriate dimensions to assess the effect. However, if 15 μm in the major dimension is chosen as an approximation to critical, we find that the core, intermediate and rim zones have respectively 37, 50 and 43% of inclusions larger than the critical dimension. Therefore not less than 50% of the inclusions in each zone would decrepitate at a temperature above the predicted temperature. Nevertheless, it is observed that the decrepitation peaks are only displaced slightly above their predicted positions. It seems likely therefore that either the acoustic emissions from very small inclusions are below background, or that their decrepitation is postponed until effective weakening of the crystal occurs, associated with the α-β phase transition at 573°C.

The change in relative intensity of the low and intermediate temperature peaks of the core samples with particle size (Table 1, Fig. 5) is an interesting feature of the data. The relative intensity of the low to the intermediate peak is similar for the coarser three fractions and even appears to increase slightly with decrease in particle size, but for the 106-212 and 53-106 μm fractions there is a significant decrease in the ratio. The changes in the positions of the means of these two peaks are small and probably not significant. There appear to be two possible explanations for these results. Either the average size of the inclusions giving rise to the low temperature peak is relatively large so that they are eliminated from the quartz more rapidly as the particle size is decreased, or the healed fractures that host the low temperature inclusions are preferentially re-opened on crushing.

Conclusions

It has been possible to show that heating stage homogenization temperature data and decrepitation data for fluid inclusions are closely correlated, confirming that the observed acoustic emission does originate in the fluid inclusions. The correction procedures used appear to be successful in deriving an approximate mean homogenization temperature (Thm) from the mean decrepitation temperature (Tdm) at least in those quartz samples in which most of the inclusions are larger than the critical dimension of about 15 μm diameter.

Acknowledgements

We would like to acknowledge the continuing interest and involvement of Mr Kingsley Burlinson in this project, and assistance in the data collection by Ms Judith Bryce.

References

ANDREWS, E.C. (1916): The molybdenum industry in New South Wales. - Mineral Resources of N.S.W. No. 24, 199pp.

BURLINSON, K., DUBESSY, J.C., HLADKY, G. & WILKINS, R.W.T. (1983): The use of fluid inclusion decrepitometry to distinguish mineralized and barren quartz veins in the Aberfoyle tin-tungsten mine area, Tasmania. - J. Geochem. Explor. 19, 319-333.

EADINGTON, P.J. (1977): A study of fluid inclusions and their significance in minerals from hydrothermal ore deposits, New England, New South Wales. Ph.D. Thesis, University of Newcastle, Australia, 235pp.

GARRETY, M.D. (1953): Bismuth-molybdenite pipes of New England. - In: Geology of Australian Ore Deposits (EDWARDS, A.B., Ed.). Fifth Mining and Metallurgy Congress, Vol. 1. Australasian Institute of Mining and Metallurgy, Melbourne, pp.962-967.

HLADKY, G. & WILKINS, R.W.T. (1987): A new approach to fluid inclusion decrepitometry. Practice. - Chem. Geol. 61, in press.

LAWRENCE, L.J. & MARKAM, N.L. (1962): A contribution to the study of the molybdenite pipes of Kingsgate, N.S.W., with special reference to ore mineralogy. - Proc. Australas. Inst. Min. Metall. 203, 67-94.

SCOTT, H.S. (1948): The decrepitation method applied to minerals with fluid inclusions. - Econ. Geol. 43, 637-645.

SMITH, F.G. (1949): A method of determining the direction of flow of hydrothermal solutions. - Econ. Geol. 45, 62-69.

WILKINS, R.W.T., HLADKY, G. & EWALD, A. (1987): A new approach to fluid inclusion decrepitometry. Fundamentals. - In preparation.

Figure captions

Fig. 1. Section of the Kingsgate quartz crystal showing the location of samples selected for study.

Fig. 2. Size distribution of 200 fluid inclusions in samples from the three zones of the Kingsgate quartz crystal.

Fig. 3. Ice melting points for inclusions from the three growth zones of the Kingsgate quartz cyrstal. Shading denotes data from inclusions in which gas hydrates were also observed.

Fig. 4. Comparison of homogenization temperatures obtained from heating-freezing stage examination of thin sections (left of diagram) and decrepitation data from crushed samples (right of diagram) from the three growth zones of the Kingsgate quartz crystal.

Fig. 5. Decrepigrams of different size fractions of the crushed core zone sample from the Kingsgate quartz crystal.

Table 1. Decrepitation results for different size fractions of crushed samples from three growth zones of the Kingsgate quartz crystal.

Sample	Grain size (μm)	Total count	Low-temperature peak		Intermediate-temperature peak		Phase- transition peak	
			Count	Mean temp. (°C)	Count	Mean temp. (°C)	Count	Mean temp. (°C)
Rim	600 - 1000	17768	13392	368.9	-	-	3874	548.6
	425 - 600	22161	16553	371.5	-	-	5216	545.7
	212 - 425	19408	14129	377.2	-	-	4998	547.1
	106 - 212	14095	9479	382.6	-	-	4383	547.1
	53 - 106	4661	2843	386.3	-	-	1527	548.5
Inter-mediate	600 - 1000	18134	14101	380.7	-	-	3407	548.2
	425 - 600	20189	15539	385.2	-	-	4098	545.8
	212 - 425	18622	13896	389.4	-	-	4200	545.8
	106 - 212	11308	8120	399.1	-	-	2843	549.7
	53 - 106	4021	2656	404.3	-	-	959	550.7
Core	600 - 1000	50614	19724	377.9	26138	460.2	3944	545.2
	425 - 600	47010	18485	386.2	23461	464.9	3359	545.9
	212 - 425	53726	21741	395.5	26279	466.1	4862	545.2
	106 - 212	31467	9674	403.1	18849	468.0	2898	548.8
	53 - 106	13708	2564	388.4	9945	464.2	1291	548.4

Table 2. Comparison of measured mean decrepitation (Tdm) and homogenization (Thm) temperatures of fluid inclusions in growth zones of a quartz crystal from Kingsgate with estimated Thm values for a range of fluids similar to those found in the inclusions. Tdm data are from the 425-600 μm fraction.

Zone in crystal	Tdm measured (°C)	Thm measured (°C)	Thm estimated (°C)			
			General correction −75 ± 20°C	Corrected for H_2O	Corrected for 1% NaCl	Corrected for 5% NaCl
Rim	371	260	296 ± 20	296	292	297
Inter-mediate	385	276	310 ± 20	310	303	308
Core	386	~300	311 ± 20	311	304	309
	465	~350	390 ± 20	357	362	370

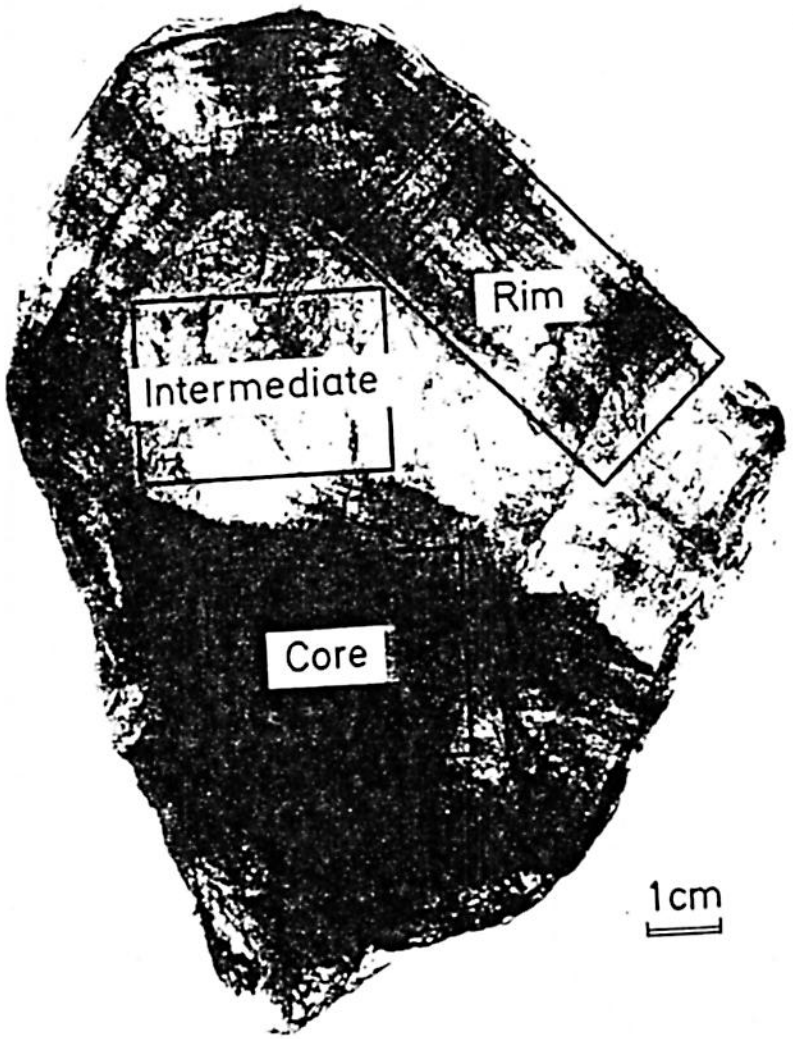

Fig. 1.

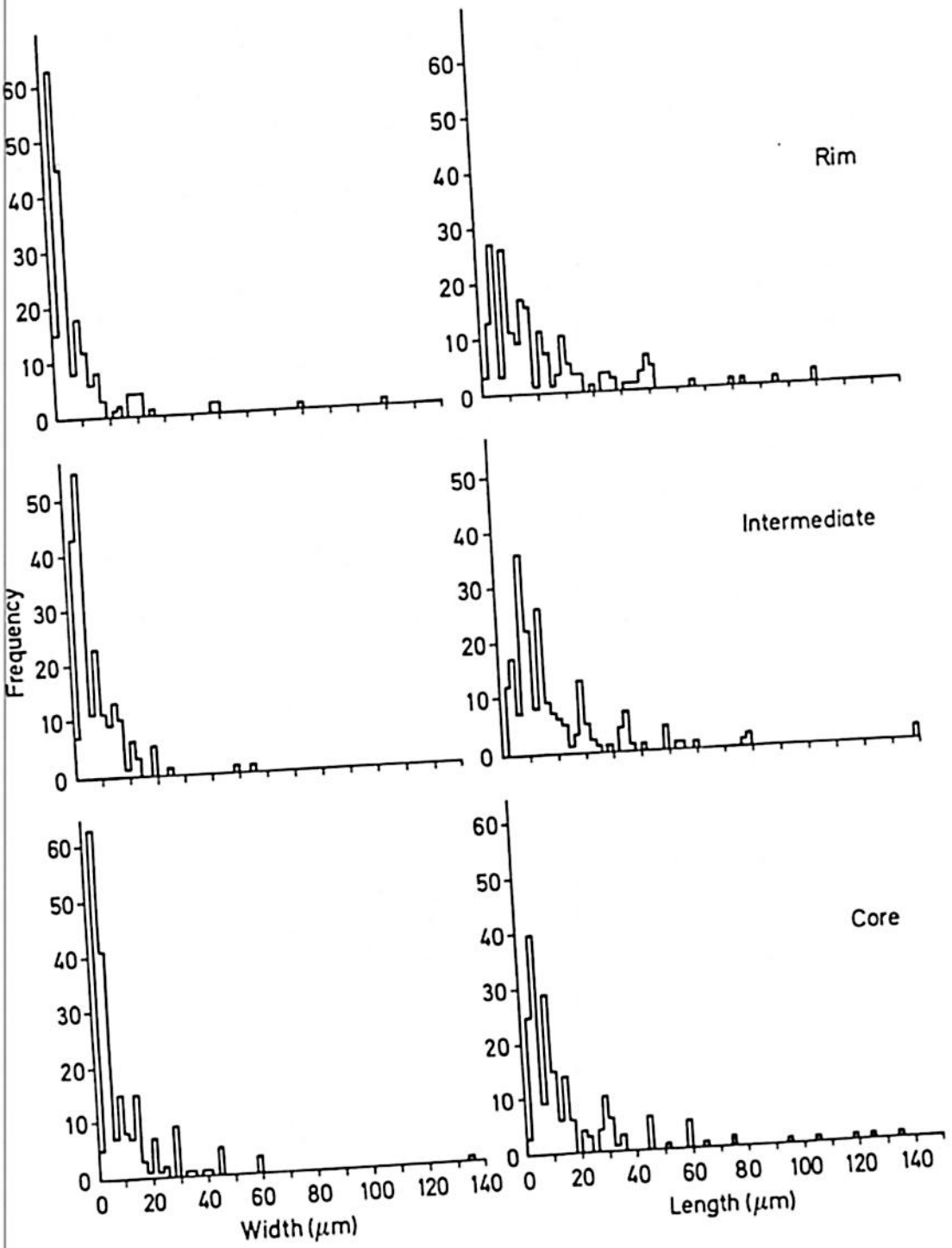
Rim
Intermediate
Core
Frequency
Width (μm)
Length (μm)
0
10
20
30
40
50
60
0
20
40
60
80
100
120
140

Fig. 2.

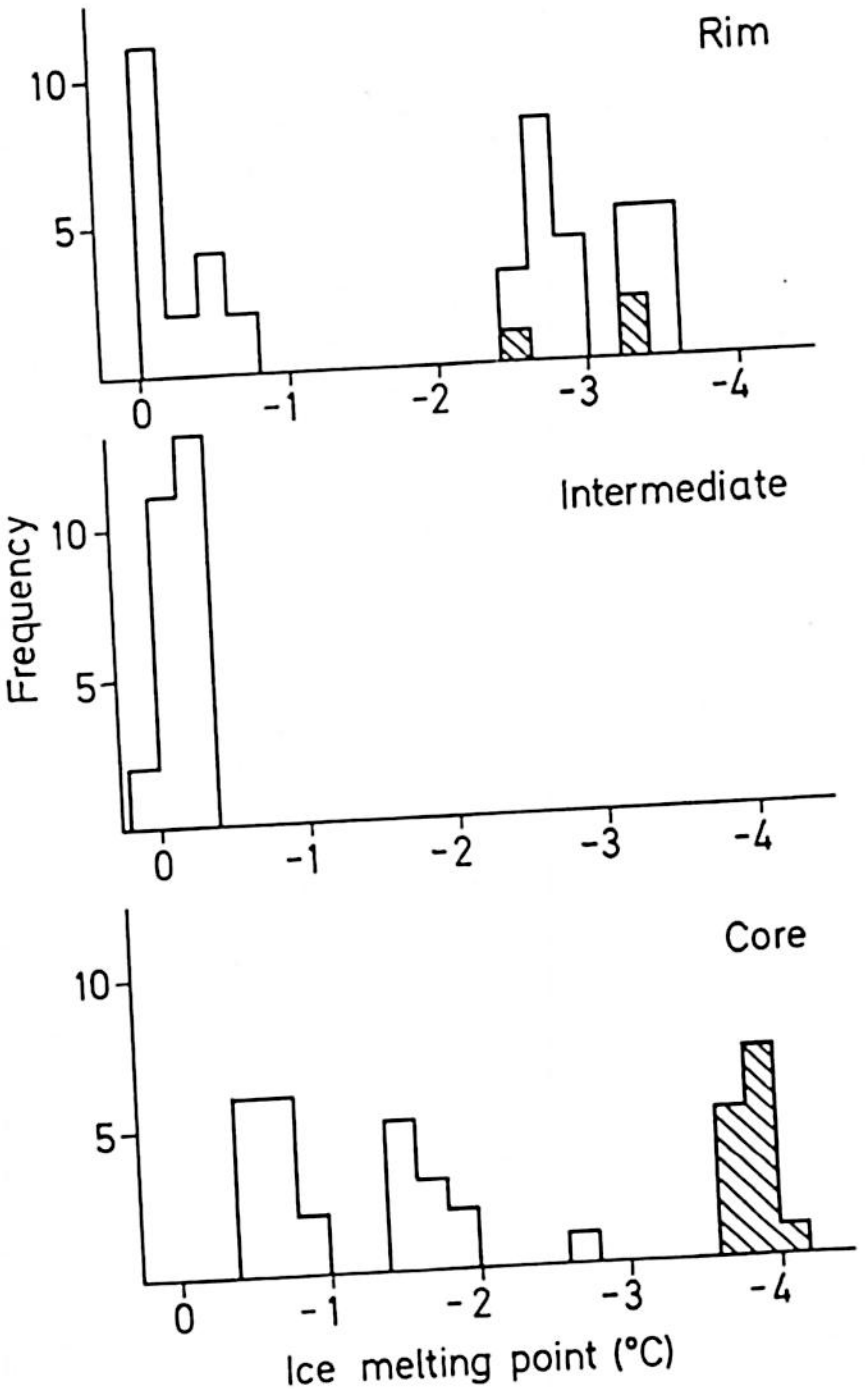
Rim
10
5
0
-1
-2
-3
-4
Intermediate
Frequency
10
5
0
-1
-2
-3
-4
Core
10
5
0
-1
-2
-3
-4
Ice melting point (°C)

Fig. 3.

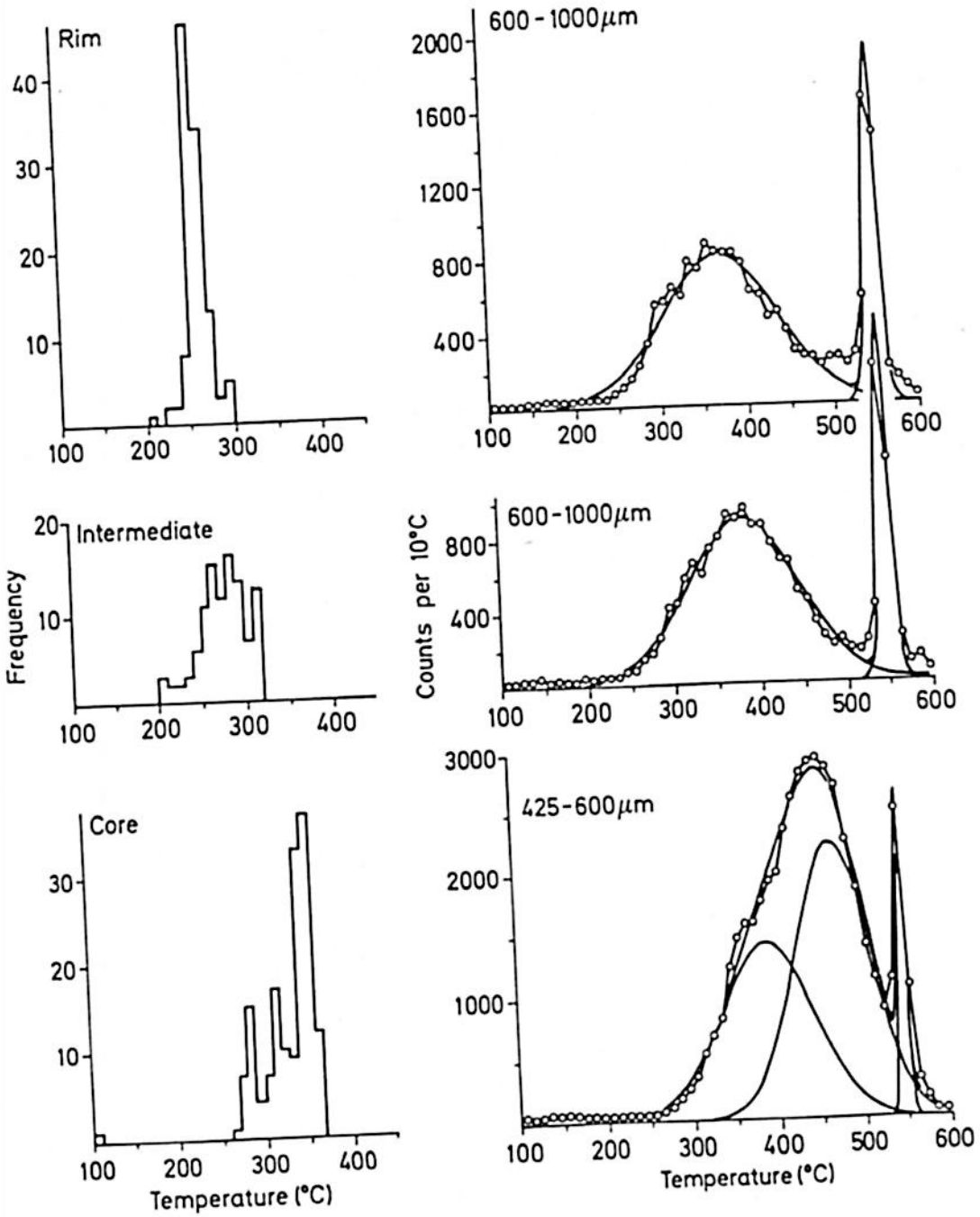
Rim
Intermediate
Core
Frequency
600-1000μm
600-1000μm
425-600μm
Counts per 10°C
Temperature (°C)

Fig. 4.

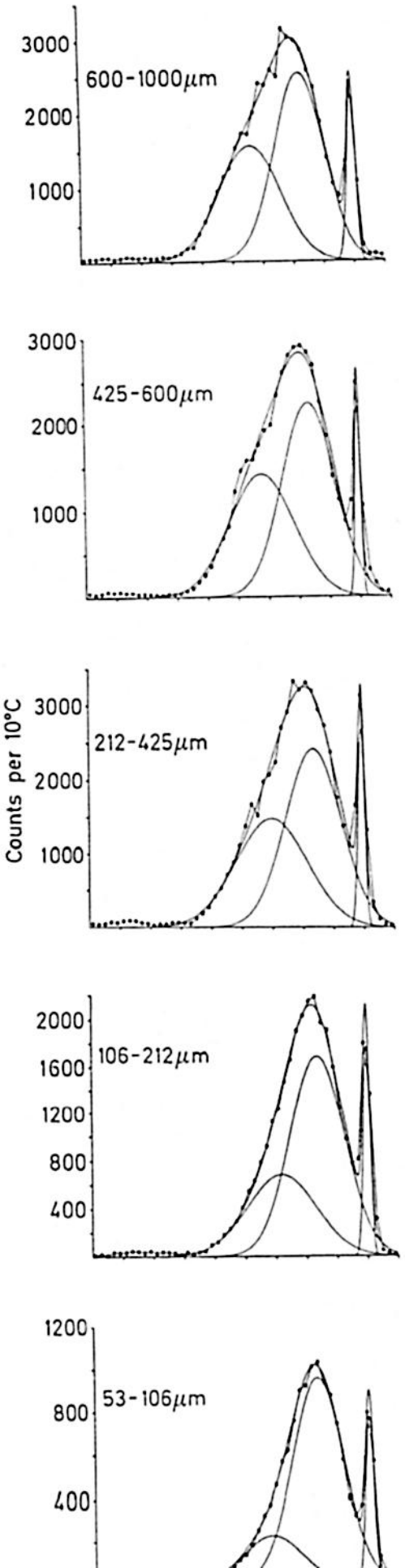
600-1000μm
425-600μm
212-425μm
106-212μm
53-106μm
Counts per 10°C
3000
2000
1000
1600
1200
800
400

Fig. 5.